Thermochimica Acta 472 (2008) 11–16

Contents lists available at ScienceDirect

Thermochimica Acta

journal homepage: www.elsevier.com/locate/tca

Isothermal crystallization kinetics of isotactic polypropylene with inorganic fullerene-like WS_2 nanoparticles

Mohammed Naffakh[a,*], Zulima Martín[a], Carlos Marco[a], Marián A. Gómez[a], Ignacio Jiménez[b]

[a] *Departamento de Física e Ingeniería de Polímeros, Instituto de Ciencia y Tecnología de Polímeros, CSIC, C/Juan de la Cierva, 3, 28006 Madrid, Spain*
[b] *Instituto de Ciencia de Materiales de Madrid, CSIC, Campus de Cantoblanco, 28049 Madrid, Spain*

ARTICLE INFO

Article history:
Received 23 January 2008
Received in revised form 5 March 2008
Accepted 10 March 2008
Available online 18 March 2008

Keywords:
Inorganic fullerene nanoparticles
Isotactic polypropylene
Nanocomposites
Crystallization kinetics

ABSTRACT

Nanometric-sized inorganic fullerene-like tungsten disulfide particles (IF-WS_2) were used to produce new isotactic polypropylene (iPP) nanocomposites. A remarkable increase of the crystallization rate of iPP in the nanocomposites was observed by DSC and X-ray diffraction techniques using synchrotron radiation. This fact was related to the high nucleation efficiency of IF-WS_2 nanoparticles on the α-form crystals of iPP. Other parameters such as the Avrami exponent, the equilibrium melting temperature, and the fold surface free energy of crystallization of iPP chains in the nanocomposites were obtained from the calorimetric data in order to determine the effect of the nanoparticles on them. A decrease in the fold surface free energy was calculated with increasing IF-WS_2 content.

1. Introduction

Isotactic polypropylene (iPP) is a versatile thermoplastic polymer which is used in many technical applications in large volume. Due to its easy processability, good mechanical properties, great recyclability, and low cost, iPP has found a wide range of applications in areas like packaging, households and automobiles. However, it exhibits a relatively low modulus and stiffness compared to engineering plastics. Reinforcement of iPP with nanometer-scale inorganic particles to enhance its properties, especially the mechanical ones, and which may induce changes in polymer crystallization behaviour and morphology, has been attempted [1,2]. On the other hand, the use of nucleating agents for iPP is very extensive and finds importance because the control of the crystallization behaviour allows the modification of the microstructure and the enhancement of some physical properties of the polymer, such as thermal, mechanical, and optical properties. Generally, nucleating agents of iPP can be divided into α and β nucleating agents, in which α nucleating agents can improve tensile and flexural properties as well as transparency of iPP while β nucleating agents can improve impact strength and heat distortion temperature of iPP; however, β nucleating agents would decrease the stiffness of iPP [3–6].

Tungsten disulfide (WS_2) nanoparticles are a closed cage structure synthesized by the reaction of metal oxide nanoparticles with H_2S at elevated temperatures [7–9]. These non-carbon materials are normally referred to as "inorganic fullerene-like materials (IF)" [7]. The outstanding property of IF-WS_2 nanoparticles in applications such as in solid lubricants [10], catalysts [11], scanning tunneling microscopy probes [12], field emitters [13] and shock absorbing [14] has initiated many efforts to synthesize them. In a recent work, a facile large-scale and low-cost route was developed to synthesize IF-WS_2 nanoparticles [15]. The excellent lubricating performance of the IF-WS_2 was attributed to their small size, closed hollow structure and chemical inertness, which will bring a wide spectrum of possible applications, especially as promising candidates for the preparation of advanced polymer nanocomposites [16]. In particular, inclusion of IF-WS_2 nanoparticles with new structures in polymer matrices combines the flexibility of the polymer with the high modulus and low friction of this inorganic compound leading to improved mechanical properties of the polymer matrix, as it has been reported in a recent work using an epoxy resin and polyacetal [17]. However, to control the mechanical and various other properties of the nanocomposites during processing, it is essential to know the crystallization behaviour of the polymer in detail (crystalline structure, crystallization rate, overall crystallinity, size of crystallites, etc.) and also how it is affected in the presence of nanoparticles.

We have previously reported on the preparation, morphology and some thermal and mechanical properties of iPP/IF-WS_2

* Corresponding author. Tel.: +34 915622900; fax: +34 915644853.
E-mail address: mnaffakh@ictp.csic.es (M. Naffakh).

0040-6031/$ – see front matter © 2008 Elsevier B.V. All rights reserved.
doi:10.1016/j.tca.2008.03.003

nanocomposites [16]. In this work we have focused on the analysis of the isothermal crystallization behaviour of the new nanocomposites. The effect of IF-WS_2 nanoparticles on the isothermal crystallization kinetics of iPP has been investigated in detail. There are four main aspects which have been studied, i.e., (1) whether the IF-WS_2 alters the crystal form of iPP, (2) whether the presence of IF-WS_2 influences the crystallization regime of iPP, (3) whether IF-WS_2 affects the crystallization rate and fold surface free energy of iPP during crystallization and (4) whether IF-WS_2 influences the subsequent melting behaviour of iPP.

2. Experimental

2.1. Materials and processing

The polypropylene studied was an isotactic homopolymer provided by REPSOL-YPF (Spain). It is characterized by an isotacticity of 95% determined by solution NMR and a viscosity average molecular weight of 164,700 g mol^{-1} [18]. The IF-WS_2 nanoparticles with an average diameter of 80 nm are commercialized as NanoLub™ and were provided by Nanomaterials (Israel) and ApNano Materials (USA). The iPP/IF-WS_2 nanocomposites containing different concentration of IF-WS_2 (0.1–2 wt.%) were prepared in a Haake Rheocord 90 system by controlling the test parameters, i.e. temperature, mixing time and rotor speed. A temperature of 210 °C, mixing time of 10 min and a rotor speed of 150 rpm were selected as standard conditions according to the morphology studies by scanning electron microscopy (SEM) [16].

2.2. Differential scanning calorimetry (DSC)

The isothermal crystallization behaviour of iPP/IF-WS_2 nanocomposites was investigated by use of the PerkinElmer DSC7/UNIX/7DX differential scanning calorimeter. All DSC operations were carried out in a nitrogen atmosphere. Samples weights were 11–12 mg and all samples were heated to 210 °C and held in the molten state for 5 min to erase their thermal history. Then the sample melts were subsequently cooled at 64 °C min^{-1} to the predetermined crystallization temperature T_c and maintained until the crystallization of the matrix was completed. From the enthalpy evolution during crystallization the kinetics of crystallization was evaluated. Partial areas, corresponding to a given percentage of the total transformation, were determined from the data points stored, for each isothermal run on a PE 7700 computer, using Pyris DSC7 kinetic software. After the completion of crystallization, the melting temperatures were determined by heating the samples at a rate of 5 °C min^{-1}. The melting enthalpy of a 100% crystalline polypropylene (ΔH_m°) was taken as 177 J g^{-1} [19].

2.3. X-ray diffraction

Wide-angle X-ray scattering (WAXS) experiments using synchrotron radiation were performed at the A2 beamline of the HASYLAB synchrotron facility (DESY, Hamburg). The experiments were performed with monochromatic X-rays of 0.15 nm wavelength using a germanium single crystal as the dispersing element. The scattering was detected with a linear Gabriel detector. All scattering intensity profiles were corrected for sample absorption, background scattering and incident beam fluctuation. The methodology used in the dynamic crystallization experiments of the nanocomposites by WAXS is similar to that described for the calorimetric experiments. Measurements were performed with acquisition time of 15 or/and 30 s for each pattern depending on the total crystallization time.

3. Results and discussion

3.1. Isothermal crystallization of iPP nanocomposites

In our previous work, nanocomposites based on isotactic polypropylene (iPP) and IF-WS_2 nanoparticles were successfully prepared via melt processing and the crystallization process under non-isothermal conditions was also studied [16]. The incorporation of IF-WS_2 on iPP matrix at the nanoscale was very effective, as observed in the morphological studies, and improved some thermal and mechanical properties. Related to the crystallization behaviour realized under dynamic condition, the crystallization temperature of iPP increased significantly with the IF-WS_2 content up to a level of 2 wt.% IF-WS_2, and at a lower rate above this value. This increase was accompanied by an increase of crystallinity. The nucleating efficiency of IF-WS_2 nanoparticles on the dynamic crystallization of α-phase of iPP reached very high values (60%–70%), the highest values observed hitherto for polypropylene nanocomposites. Taking into account these results, isothermal crystallization studies of iPP and the iPP/IF-WS_2 nanocomposites (0.1, 1 and 2 wt.% IF-WS_2) were carried out at various temperatures. As an example, the DSC crystallization exotherms of iPP/IF-WS_2 nanocomposites with 1% content of IF-WS_2 are shown and compared with pure iPP in Fig. 1. In all cases, it was observed that as the undercooling (i.e., the difference between the melting and crystallization temperature) decreases, the crystallization rate is reduced and the exothermal peak becomes broader. Thus, the induction time of the exotherm increases. In the analysis of the influence of IF-WS_2 content on crystallization behaviour of iPP, it was clearly observed that the peaks of iPP/IF-WS_2 nanocomposites are all narrower than that of pure iPP, i.e., the presence of IF-WS_2 decreases the crystallization time of iPP chains remarkably. However, the most relevant difference was the increase in the temperature range in which crystallization took place even in the presence of 0.1 wt.% of IF-WS_2 over similar timescales. In the case of iPP, the interval was between 120 and 136 °C and in the case of iPP/IF-WS_2, this interval shifts to higher crystallization temperatures (130–146 °C). However, the crystallinity values of iPP in the nanocomposites, derived from the exothermic curves, are found to be almost independent of IF-WS_2 content (54.6 ± 1%). Therefore, it can be concluded that the incorporation of the IF-WS_2 increased the crystallization rate of iPP chains without increasing the level of crystallinity developed. However, when iPP was crystallized under dynamic condition, the effect of IF-WS_2 on crystallinity was more pronounced [16]. The effect of the acceleration of the isothermal crystallization process is evident in Fig. 2 in which the crystalline conversion (θ) in iPP/IF-WS_2 nanocomposites are plotted as a function of time at a fixed crystallization temperature.

The isothermal crystallization kinetics of polypropylene and its composites was analyzed in terms of the well known Avrami equation, which provides a convenient approach to analyze the overall crystallization kinetics and its logarithmic form which is expressed as [20,21]:

$$\log[-\ln(1-\theta_t)] = \log k_n + n \log t \quad (1)$$

where θ_t is the crystalline conversion at time 't', k_n is the kinetic growth rate constant and n is the Avrami exponent related to the type of nucleation and to the geometry of the growing crystals. Fig. 3 shows the typical Avrami plots ($\log[-\ln(1-\theta_t)]$ *vs.* $\log t$) corresponding to iPP/IF-WS_2 nanocomposites. Linear regression of these straight lines at low degrees of crystalline transformation (5%–30%) yielded the Avrami exponents (n).

According to the nucleation and growth mechanism, the Avrami exponent n should be an integer value. However, the values of n reported in the literature are dispersed, ranging from 1.8 to 4

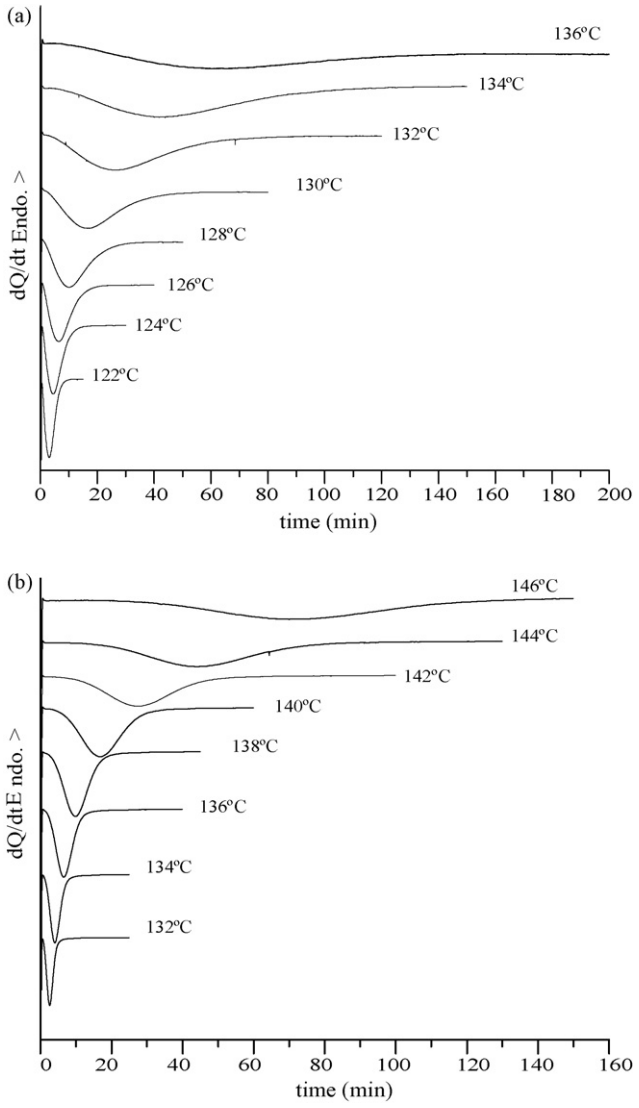

Fig. 1. DSC thermograms of isothermal crystallization of (a) iPP and (b) iPP/IF-WS_2 (1 wt.%) nanocomposite at various temperatures.

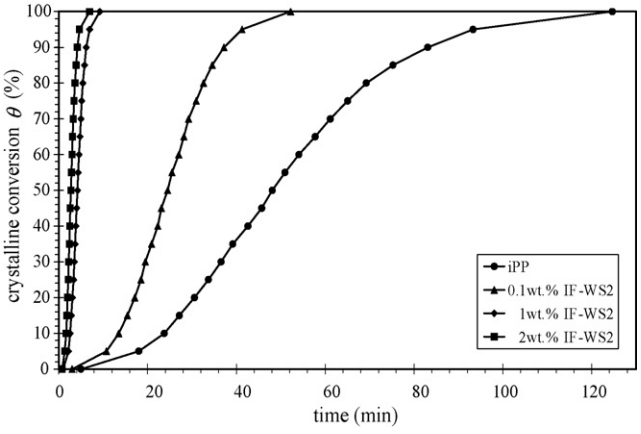

Fig. 2. Crystalline conversion (θ) of iPP/IF-WS_2 nanocomposites at T_c = 134 °C.

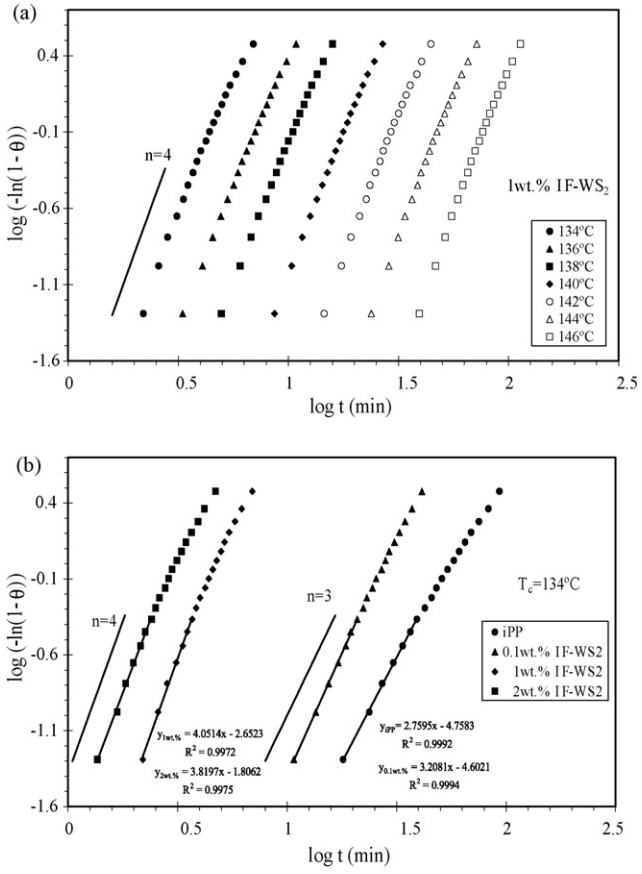

Fig. 3. Avrami plots of the crystallization of iPP/IF-WS_2 nanocomposites as a function of (a) the crystallization temperature and (b) the composition.

[22]. These non-integer values are caused by some characteristics of polymers not matching the simplification in the Avrami equation, such as secondary crystallization process, mixed nucleation modes and the change in material density [23]. Moreover, even some experimental factors such as an error introduced in the determination of zero point of crystallization and the melting residence time can lead to non-integer values of n [18,24].

In our case, a value of n of 3 ± 0.2 was obtained for pure iPP over the crystallization temperature range studied in agreement with previous work [25]. This value can be attributed to a homogenous nucleation with two-dimensional growth. However, in the case of nanocomposites, the n values are 3 ± 0.4 for iPP/IF-WS_2 (0.1 wt.%) and 4 ± 0.2 for iPP/IF-WS_2 (1 wt.%) and iPP/IF-WS_2 (2 wt.%), respectively. The increase in the n exponent with increasing the IF-WS_2 content can be attributed to a change from two-dimensional to three-dimensional crystal growth of the polymer matrix.

In this work, the analysis of the crystallization kinetics was undertaken by the determination of the overall crystallization rate, with both stages of the crystallization process considered (i.e., nucleation and growth). Thus, the global rate (G) could be calculated as:

$$G \approx \frac{1}{\tau_i} \tag{2}$$

over the time necessary for the crystallization of polymers, where G can be directly determined from the time necessary to reach a pre-established degree of crystalline transformation (i) denominated τ_i, and from its variation with the T_c, for a predetermined molecular weight.

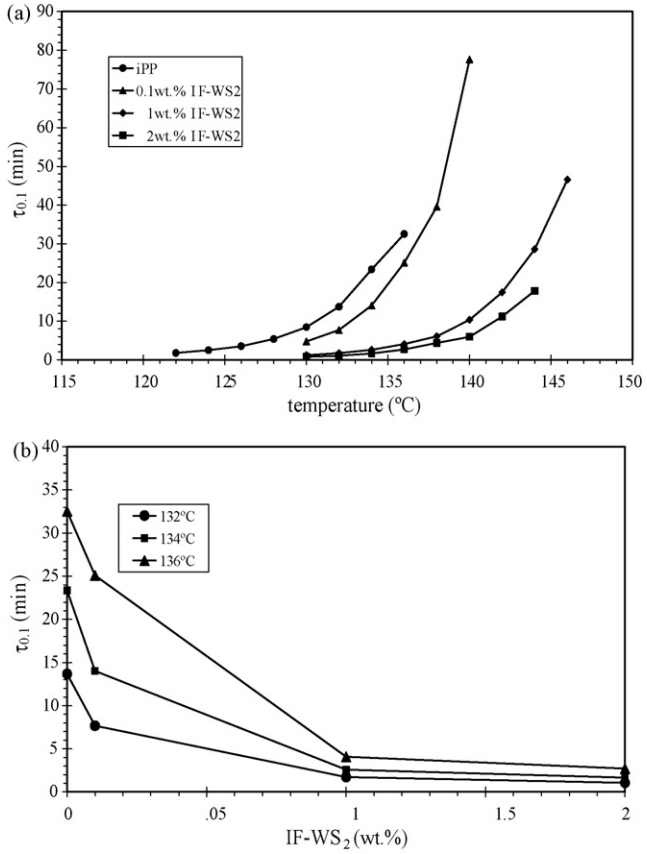

Fig. 4. Time to reach the 10% degree of transformation ($\tau_{0.1}$) of iPP/IF-WS_2 nanocomposites as a function of (a) the crystallization temperature and (b) the composition.

The rate constant of the crystallization process (k_n) can be determined by the following expression [26]:

$$k_n = \frac{\ln 2}{(\tau_{0.5})^n} \quad (3)$$

where $\tau_{0.5}$ is the time necessary to reach 50% of crystalline transformation and the values of the exponent n are associated with each T_c.

Fig. 4 shows the changes in the time to reach 10% of transformation ($\tau_{0.1}$) for iPP/IF-WS_2 nanocomposites as a function of the crystallization temperature and the composition. In all cases, the values of $\tau_{0.1}$ increased exponentially with temperature, (Fig. 4a), confirming that the ordering process occurred through a nucleation mechanism. Our second observation was the important increase in the range of crystallization temperature in which iPP crystallized for a similar level of crystalline transformation, which led to a progressive reduction in this parameter with increasing IF-WS_2 content, as shown in Fig. 4b for a T_c of 134 °C. That is, the addition of IF-WS_2 produces an increase in the crystallization rate of iPP for each T_c as the concentration of IF-WS_2 is increased.

This effect is also observed in the corresponding values of the global rate constant, k, as shown in Fig. 5 for iPP/IF-WS_2 nanocomposites. In all cases, the values of k_n for the nanocomposites were higher than iPP. Although iPP presented a k_n of around 5.08×10^{-4} for T_c of 128 °C, in the case of the nanocomposites, values of k_n of the same order could be obtained at much higher T_c (137 °C for concentration of 2 wt.% of IF-WS_2). The results clearly prove that the IF-WS_2 nanoparticles play the role of effective nucleating agents for iPP and promote nucleation of iPP chains at small loading of IF-WS_2 during isothermal crystallization.

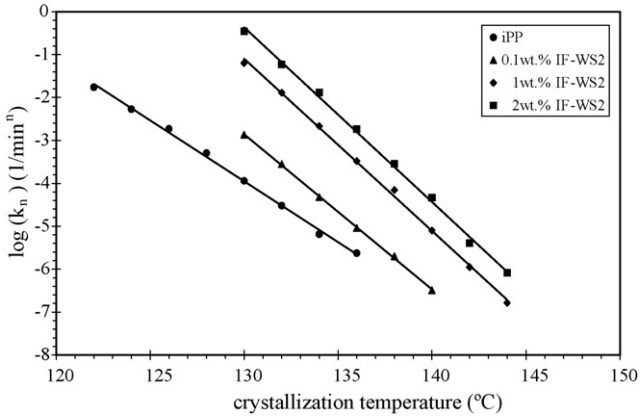

Fig. 5. Logarithmic plots of the rate constant (k_n) of iPP/IF-WS_2 nanocomposites as a function of crystallization temperature (T_c).

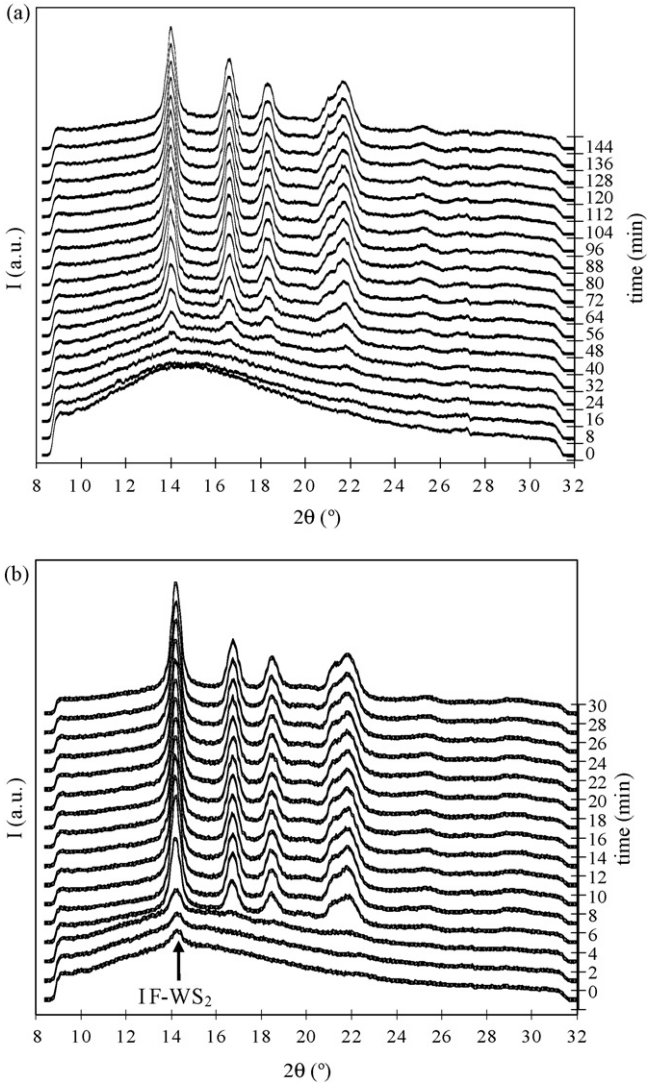

Fig. 6. WAXS patterns of (a) iPP and (b) iPP/IF-WS_2 (1 wt.%) nanocomposite crystallized at 134 °C.

3.2. Crystal structure of iPP nanocomposites

To determine the nanocomposite structure, WAXS experiments using synchrotron radiation were performed. Fig. 6 shows the WAXS patterns of iPP and iPP/IF-WS_2 (1 wt.%) nanocomposites. It is well known that isotactic polypropylene can crystallize in different crystalline polymorphs, i.e. the monoclinic α-form, the trigonal β-form, triclinic γ-form and smetic-form. The main Bragg reflections at 2θ angles of 14°, 16.7°, 18.5° and 21.7° corresponding to the (1 1 0), (0 4 0), (1 3 0) and (1 1 1) planes of the α-form, respectively, can all be seen in the WAXS diffractograms of the nanocomposites, indicating the existence of α-form crystals of iPP and the absence of β-form crystals. It can be concluded that the presence of IF-WS_2 nanoparticles does not affect the crystalline polymorph of iPP. However, the crystallization rate of iPP is accelerated by the addition of IF-WS_2, as shown in the development of the WAXS crystalline reflections as function of the crystallization time.

3.3. Melting behaviour and equilibrium melting points

Fig. 7 presents the melting behaviour of isothermally crystallized iPP/IF-WS_2 nanocomposites at different crystallization temperatures. The melting profile of iPP and iPP/IF-WS_2 nanocomposites appears as two melting endotherms, a broad and poorly defined shoulder at lower temperatures (T_{mI}) and a well-defined maximum at higher temperature (T_{mII}). Its is clearly observed that all melting temperatures shift to higher values with increasing T_c, which is directly related to the perfections of the crystals formed at higher crystallization temperatures (i.e., low undercooling). In our case, we do not exclude the existence of melting-recrystallization-melting phenomena during heating, as reported previously in the same iPP matrix nucleated with sorbitol derivatives [25].

The kinetic data obtained by calorimetry were also analyzed from a thermodynamic point of view. Plots T_m *vs.* T_c are shown in Fig. 8. It can be seen that, in the range of T_c analyzed, the data of T_m showed no evidence for any influence of the composition in the double melting endotherms, except that of an expected increase in the melting temperatures with the crystallization temperature. The extrapolation of the variation of apparent melting temperature (T_{mII}) to the line corresponding with $T_m = T_c$ with little dispersion led to a global value of 196 °C, which can be considered the T_m° of the iPP/IF-WS_2 nanocomposites. These results are in agreement with other works [25,27], which point towards the influence of the nucleating agent on the crystallization rate but not on the melting temperature in the thermodynamic equilibrium (T_m°).

3.4. Crystallization activation energy

The crystallization thermodynamics and kinetics of the nanocomposites have been analyzed on the basis of the theory of Lauritzen and Hoffman (LH) [28,29]. Accordingly, the spherulitic growth rate (G), defined as $G = 1/\tau_{0.1}$, is given as a function of the crystallization temperature (T_c) by the following bi-exponential equation:

$$G = G_0 \exp\left[-\frac{U^*}{R(T_c - T_0)}\right] exp\left[-\frac{K_g}{fT_c\Delta T}\right] \quad (4)$$

where G_0 is a constant independent of temperature, R is the universal gas constant, U^* is the energy of the chain transport in the melt, T_0 is the temperature below which there is no chain motion (usually $T_0 = T_g - 30$ K), and T_c is the crystallization temperature. $\Delta T = T_m^\circ - T_c$ is the supercooling range (T_m° is the equilibrium melting temperature), f is the corrective factor that takes into account the variation of equilibrium melting enthalpy (ΔH_m°) with temperature, defined as $2T_c/(T_c + T_m^\circ)$ and K_g is the term connected with

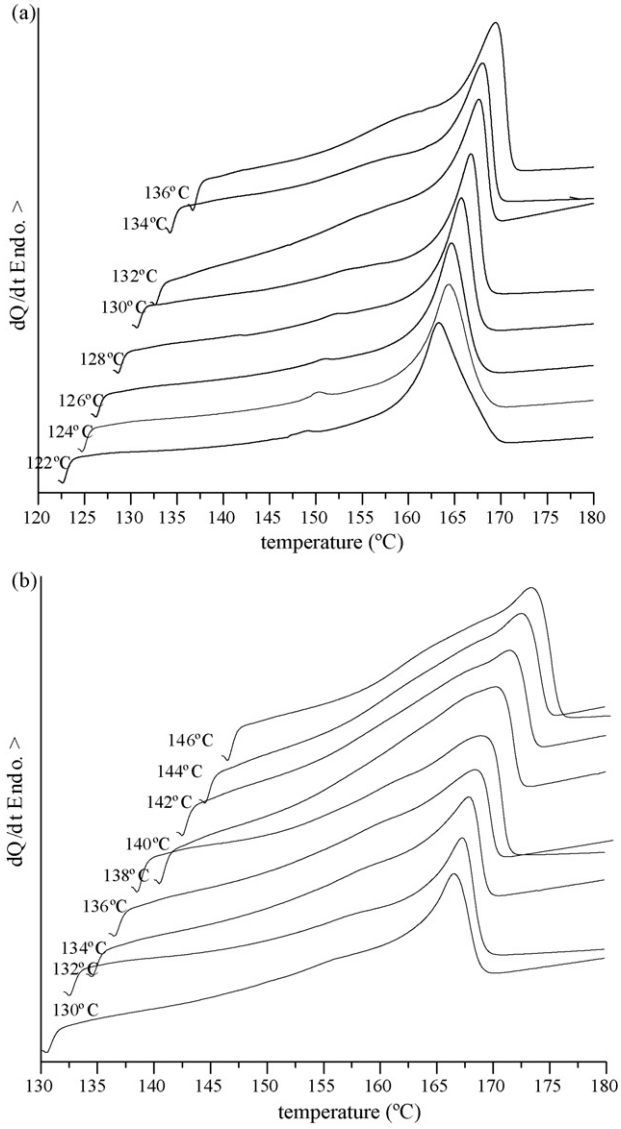

Fig. 7. Melting DSC thermograms of (a) iPP and (b) iPP/IF-WS_2 (1 wt.%) nanocomposite obtained at a heating rate of 5 °C min^{-1} after isothermal crystallization at the indicated temperatures.

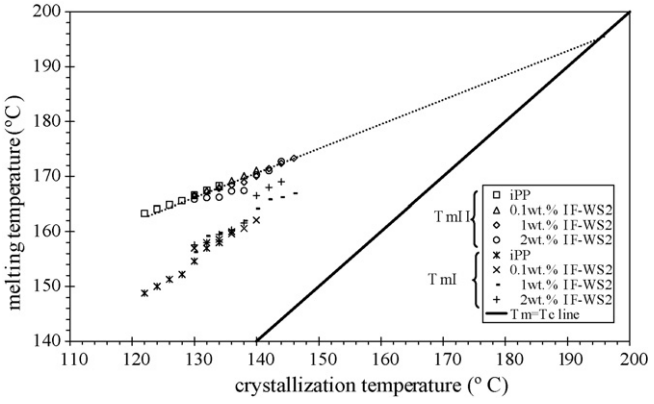

Fig. 8. Plots of the observed melting temperature (T_m) of iPP/IF-WS_2 nanocomposites as a function of crystallization temperature (T_c).

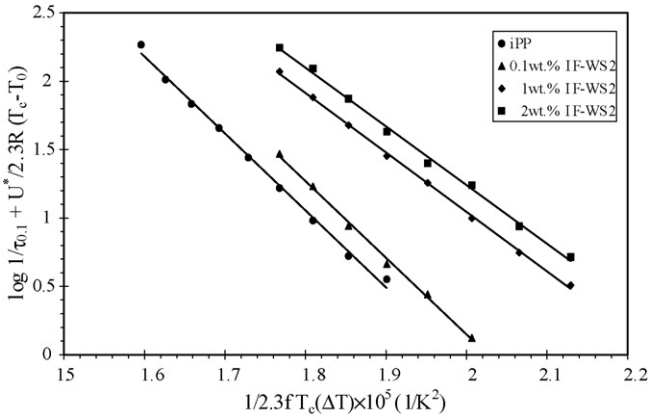

Fig. 9. Lauritzen–Hoffman plots of iPP/IF-WS_2 nanocomposites.

the energy required for the formation of the nuclei of critical size and can be expressed as:

$$K_g = \frac{jb_0\sigma\sigma_e T_m^0}{k_B \Delta H_m^0} \quad (5)$$

where j is a variable that considers the crystallization regime and assumes the value $j = 4$ for regimes I and III and $j = 2$ for regime II [30], σ and σ_e are the free energies per unit area of the surfaces of the lamellae parallel and perpendicular to the chain direction, respectively, b_0 is the distance between two adjacent fold planes and k_B is the Boltzmann constant. The values of U^*, T_0, R, k_B, T_m°, b_0, ΔH_m°, and σ are 6280 J mol^{-1} [30], 250 K [16], 8.32 J mol^{-1} K^{-1}, 1.3810^{-16} erg K^{-1}, 469 K [this work], 6.26 A [30], 177 J g^{-1} [19], and 11.5 erg cm^{-2}, respectively [30].

Fig. 9 presents the above LH plots of iPP/IF-WS_2 nanocomposites in terms of Eq. (4) and shows that the experimental data can be reasonably fitted with straight lines. According to T_c (124–136 °C), the crystallization of iPP occurred in crystallization regime III [30]. It is also noticed in Fig. 9 that there is no change in the slopes for the nanocomposites, implying that no regime transition occurs in the crystallization temperature range of nanocomposites. From the slope of LH plots, the values of K_g were calculated and the values of σ_e were obtained from $\sigma\sigma_e$ by substituting K_g into Eq. (5). The value of σ_e of iPP is 91.9 erg cm^{-2}. With the addition of IF-WS_2, the value of σ_e changed to 91.6 erg cm^{-2} at 0.1 wt.% IF-WS_2 content, 71.0 erg cm^{-2} at 1 wt.% IF-WS_2 content and 70.1 erg cm^{-2} at 2 wt.% IF-WS_2 content, respectively. There is a clear tendency for σ_e to decrease as the IF-WS_2 content is increased. As is well known, a foreign surface frequently reduces the nucleus size needed for crystal growth since the creation of the interface between the polymer crystal and substrate may be less hindered than the creation of the corresponding free polymer crystal surface [31]. Based on the results of iPP/IF-WS_2 nanocomposites, we conclude that the addition of IF-WS_2 nanoparticles reduces the work needed to create a new surface, hence leading to faster crystallization rates.

4. Conclusions

The effect of IF-WS_2 nanoparticles on the crystal structure and the isothermal crystallization behaviour of iPP in their nanocomposites were studied. X-ray diffraction results indicated that the addition of IF-WS_2 nanoparticles did not alter the crystalline structure of iPP which crystallized in the nanocomposites in the monoclinic α-form. Under isothermal conditions, the iPP nanocomposites exhibited higher crystallization rates than pure iPP and different Avrami exponents when compared with pure iPP. However, the crystallinity values of iPP/IF-WS_2 nanocomposites were found to be independent of IF-WS_2 content. The crystallization temperature interval of iPP shifts to a higher temperature with increasing the IF-WS_2 content. This fact was reflected in the melting temperature peaks of iPP/IF-WS_2 nanocomposites without changing the equilibrium melting temperature of iPP. In addition, in the analysis of the activation energy of crystallization regime III of iPP/IF-WS_2 nanocomposites, it was shown that the fold surface free energy (σ_e) of iPP chains decreased with increasing IF-WS_2 content. This fact can be attributed to the high nucleating efficiency of IF-WS_2 nanoparticles on iPP.

Acknowledgements

This work was carried out under the financial support of the FOREMOST project of the European Union 6th Framework Program (contract number: NMP3-CT-2005-515840). The authors also thank the European Commission for research and travel grants for the X-ray synchrotron experiments performed at the Soft Condensed Matter A2 beamline at HASYLAB (DESY-Hamburg) under contract number: I-20060118 EC. Partial support from CICYT (NAN2004-09183-C10-02) is also acknowledged. The authors would like to thank Dr. S. Funari for his technical assistance in the synchrotron experiments. Dr. M. Naffakh would also like to express his gratitude to the Consejo Superior de Investigaciones Cientificas (CSIC) for postdoctoral contract (I3PDR-6-02), financed by the European Social Fund.

References

[1] C.M. Chan, J. Wu, J.X. Li, Y.K. Cheung, Polymer 43 (2002) 2981.
[2] S. Jain, H. Goossens, M. Van Duin, P. Lemstra, Polymer 46 (2005) 8805.
[3] P. Jacoby, B.H. Bersted, W.J. Kissel, C.E. Smith, J. Polym. Sci. Part B: Polym. Phys. 24 (1986) 461.
[4] S.C. Tjong, J.S. Shen, R.K.Y. Li, Polym. Eng. Sci. 36 (1996) 100.
[5] J. Varga, Crystallization, melting and supermolecular structure of isotactic polypropylene, Polypropylene: Structure, Blends and Composites, vol. 1, Structure and Morphology, Chapman & Hall, London, 1995, pp. 56–115.
[6] C. Marco, M.A. Gómez, G. Ellis, J.M. Arribas, Rec. Res. Dev. Appl. Polym. Sci. 1 (2002) 587.
[7] R. Tenne, L. Margulis, M. Genut, G. Hodes, Nature 360 (1992) 444.
[8] L. Margulis, G. Salitra, R. Tenne, M. Talianker, Nature 365 (1993) 113.
[9] Y. Feldman, E. Wasserman, D.J. Srolovitz, R. Tenne, Science 267 (1995) 222.
[10] L. Rapoport, Y. Bilik, Y. Feldman, M. Homyonfer, S.R. Cohen, R. Tenne, Nature 387 (1997) 791.
[11] T. Kubota, K. Sato, A. Kato, Usman, T. Ebihara, T. Fujikawa, Y. Araki, K. Ishida, Y. Okamoto, Appl. Catal. A 290 (2005) 17.
[12] A. Rothschild, S.R. Cohen, R. Tenne, Appl. Phys. Lett. 75 (1999) 4025.
[13] Y.B. Li, Y. Bando, D. Golberg, Adv. Mater. 15 (2003) 1294.
[14] Y.Q. Zhu, T. Sekine, Y.H. Li, W.X. Wang, M.W. Fay, H. Edwards, P.D. Brown, N. Fleischer, R. Tenne, Adv. Mater. 17 (2005) 1500.
[15] H. Yang, S. Liu, J. Li, M. Li, G. Peng, G. Zou, Nanotechnology 17 (2006) 1512.
[16] M. Naffakh, Z. Martín, N. Fanegas, C. Marco, M.A. Gómez, I. Jiménez, J. Polym. Sci. Part B: Polym. Phys. 45 (2007) 2309.
[17] L. Rapoport, O. Nepomnyashchy, A. Verdyan, R. Popovitz-Biro, Y. Volovik, B. Ittah, R. Tenne, Adv. Eng. Mater. 6 (2004) 44.
[18] C. Marco, M.A. Gómez, G. Ellis, J.M. Arribas, J. Appl. Polym. Sci. 84 (2002) 1669.
[19] J.X. Li, W.L. Cheung, J. Demin, Polymer 40 (1999) 1219.
[20] M. Avrami, J. Chem. Phys. 7 (1939) 1103.
[21] M. Avrami, J. Chem. Phys. 8 (1940) 212.
[22] J. Bicerano, J. Macromol. Sci. Rev. Macromol. Chem. Phys. 38 (1998) 391.
[23] S. Srinivas, J.R. Babu, J.S. Riffle, L.W. Garth, Polym. Eng. Sci. 37 (1997) 497.
[24] J. Yu, J. He, Polymer 41 (2000) 891.
[25] C. Marco, G. Ellis, M.A. Gómez, J.M. Arribas, J. Appl. Polym. Sci. 88 (2003) 2261.
[26] S.P. Kim, S.C. Kim, Polym. Eng. Sci. 31 (1991) 110.
[27] Y. Chen, M. Xu, Gaofenzi Xuebao 2 (1998) 240.
[28] J.L. Lauritzen, J.D. Hoffman, J. Appl. Phys. 44 (1973) 4340.
[29] J.D. Hoffman, R.L. Miller, Polymer 38 (1997) 3151.
[30] E.J. Clark, J.D. Hoffman, Macromolecules 17 (1984) 878.
[31] M. Mucha, Z.J. Krolikowski, J. Therm. Anal. Calorim. 74 (2003) 549.